Michigan State University

National Superconducting Cyclotron Laboratory

A SIMPLE RELATION FOR ALPHA DECAY HALF LIVES

B. ALEX BROWN

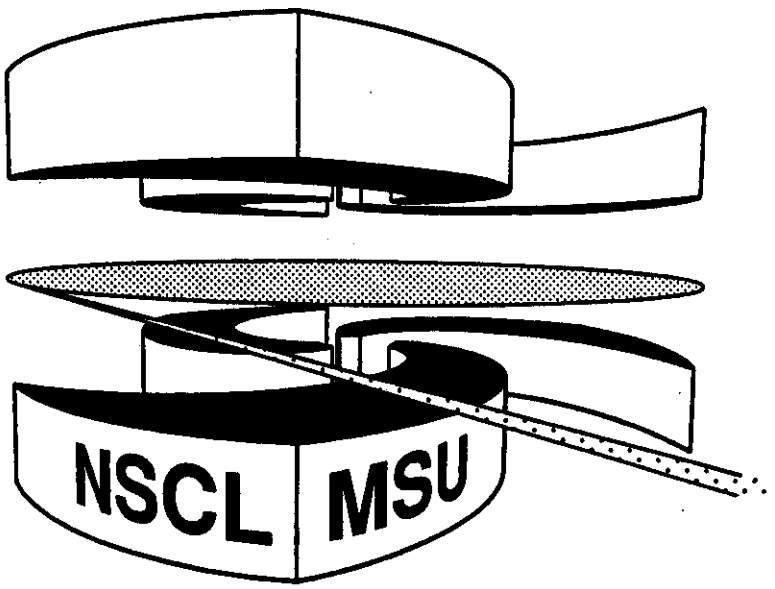

MSUCL-835

MAY 1992

MSUCL-835
May, 1992

A Simple Relation for Alpha Decay Half Lives

B. Alex Brown

National Superconducting Cyclotron Laboratory
and
Department *of Physics* and Astronomy,
Michigan State University,
East Lansing, Michigan 48824-1321, *USA*

Abstract: The experimental values of $\mathrm{Log_{10}T_{1/2}(sec)}$ plotted vs $Z_d^{0.6}/\sqrt{Q_\alpha}$ are shown to fall on a nearly universal straight line with $\mathrm{Log_{10}T_{1/2}(sec)} = (9.54\ Z_d^{0.6}/\sqrt{Q_\alpha}) - 51.37$, where Z_d is the charge number of the daughter nucleus and Q_α is expressed in units of MeV. This behavior also numerically comes out of the semi-classical WKB calculation of the harrier penetration factor. The fine structure in the ratio of experiment over theory is briefly discussed.

PACS: 23.60.+e

The earliest law for the systematics of α decay lifetimes was formulated by Geiger and Nuttall.[1] This was the observation that $\mathrm{Log_{10}T_{1/2}(sec)}$ plotted vs $1/\sqrt{Q_\alpha}$, where Q_α is the α decay Q value, empirically formed straight lines for a series of nuclei with the same charge number. In Fig. 1a, I show a modern version of this plot for the $J_i^\pi = J_f^\pi = 0^+$ α decay data tabulated in Ref 2. There are 119 data points for a range of Z_d from 74 to 106, where Z_d is the charge number of the daughter nucleus. Even though the data for a given Z_d value fall on roughly a straight line, there is a large scatter between the lines for different Z_d values.

It is well known that this trend can be understood in terms of the semi-classical approximation for the decay rate

$$W = PW_cT, \tag{1}$$

where P is the preformation probability, W_c is the collision rate of the α particle with the nuclear surface, and T is the barrier penetration factor given for ℓ=0 decays in the WKB approximation by

$$T = \exp\{-2\int_{R_t}^{R_c}\sqrt{2\mu[V(r)-Q_\alpha]/\hbar^2}\,dr\}. \tag{2}$$

In this expression R_t is the "touching" radius, $R_t = R_\alpha + R_d$, where R_α and R_d are the hard-sphere radii for the α and daughter nuclei, respectively. The potential is given by $V(r) = Z_\alpha Z_d e^2/r$, where $Z_\alpha = 2$, and R_c is the classical turning point, $R_c = Z_\alpha Z_d e^2/Q_\alpha$. The reduced mass is $\mu = M_\alpha M_d/(M_\alpha + M_d)$. Eq. (2) can be integrated exactly to give

$$T = \exp\{-2Z_\alpha Z_d e^2\sqrt{2\mu/Q_\alpha\hbar^2}\;[\cos^{-1}(x) - x\sqrt{1-x^2}]\}, \tag{3}$$

where $x = \sqrt{R_t/R_c}$. The last part of Eq. (3) can be expanded in a power series in x:

$$[\cos^{-1}(x) - x\sqrt{1-x^2}] = (\pi/2) - 2x - x^3/3\ldots. \tag{4}$$

The x^3 term is usually dropped in the discussion of this expansion, but it is important at

the level of about one order of magnitude in the half-life. The next order term in x^5 is not important at the present level of experimental and theoretical uncertainty. The barrier penetration factor in terms of the power series expansion is

$$T = \exp\{-2\sqrt{2\mu/\hbar^2}\ [\tfrac{\pi Z_\alpha Z_d e^2}{2\sqrt{Q_\alpha}} - 2\sqrt{Z_\alpha Z_d e^2 R_t}\ + \tfrac{Q_\alpha R_t^{3/2}}{3\sqrt{Z_\alpha Z_d e^2}}]\}. \tag{5}$$

The original Geiger-Nuttall rule emerges from the first term in this expansion together with the fact that the second term does not depend on Q_α. Further, as previously noted,[3] this result suggests that $\mathrm{Log_{10}T_{1/2}(sec)}$ vs $Z_d/\sqrt{Q_\alpha}$ may be a better way to plot the data. The result is shown in Fig. 1b, where the data again form lines for a fixed Z_d value, and where the scatter as a function of Z_d is somewhat less that in Fig. 1a. The scatter in Figs. 1a and 1b is due mainly to the second term on the left-hand side of Eq. (5).

Here I point out that there is a interesting interpolation between Figs. 1a and 1b. Namely, if one plots $\mathrm{Log_{10}T_{1/2}}$ vs $Z_d^{0.6}/\sqrt{Q_\alpha}$ as shown in Fig. 2a, the points fall on a nearly universal straight line. Also shown in this figure is a straight line which represents a best fit to the data. It is given by $\mathrm{Log_{10}T_{1/2}(sec)} = (9.54\ Z_d^{0.6}/\sqrt{Q_\alpha}) - 51.37$, where Q_α is expressed in units of MeV. The rms deviation of the experimental values of $\mathrm{Log_{10}T_{1/2}(sec)}$ from this straight line is 0.33. The rms deviation of the straight-line fit as a function of the power of Z_d is shown in Fig. 3 and is seen to have a sharp minimum at a value of about 0.6.

It is not obvious that this should follow from Eqs. (1), however, numerically it does. In Fig. 2b I show $\mathrm{Log_{10}T_{1/2}(sec)}$=$\mathrm{Log_{10}(ln2}/W)$ vs $Z_d^{0.6}/\sqrt{Q_\alpha}$ where W is calculated from Eq. (1) and the experimental Q_α are used. The theoretical results are compared to the best fit line from Fig. 2a. I have used $P = 1$, $R_\alpha = 2.15$ fm, $R_d = r_o A_d^{1/3}$ with $r_o = 1.2$ fm, and the classical value for W_c given by

$$W_c = (1/2R_t)\sqrt{2Q_\alpha/\mu}, \tag{6}$$

which follows from the classical motion of an α particle in the nucleus in a potential $V(r) = 0$ for $r < R_t$. (The results are, however, relatively insensitive to the value assumed for $V(r)$

inside the nucleus.) The radii R_α and R_d used above are the uniform sphere radii which are related to the rms charge radii, r_{ch} by $R = \sqrt{5/3}\, r_{ch}$ (r_{ch}=1.67 fm for the α particle). The theoretical points from the semi-classical WKB approximation follow the straight line dependence even a little better than the data (rms=0.20, see Fig. 3).

The deviation between experiment and theory can be seen in more detail in the usual way [4] by plotting the preformation factor P, as deduced from the ratio of the experimental and theoretical decay rates, vs neutron and proton number as in Fig. 4b. The well known fine structure in P vs neutron number N can easily be seen with the dominant effect being a dip to P=0.01 at $N = 126$. The top set of points in Fig. 4b obtained with a value of $r_o = 1.1$ fm illustrates the strong correlation between r_o and P. The decrease in P at $N = 126$ is correlated with a decrease in the measured rms charge radii at $N = 126$.[5] However, the radius variation is only about 2%, whereas a dip of one order of magnitude in P would require about a 10% radius change if this were the only thing responsible. Buck, Merchant and Perez [2] have postulated that the radius to be use for R_t should be determined not from the charge radius, but by the Bohr-Sommerfeld condition for an α particle wave function inside the nucleus with a fixed well depth and a fixed number of nodes. In addition, they postulate that there is a 10% increase in the number of nodes at N=126 due to the change of valence shell structure. This increases the radius by 10% and thus accounts for the discontinuity at N=126. The P values obtained from their assumption about R_t as shown in Fig. 4a, show about a factor of 2-3 improvement in the scatter, and the discontinuity at N=126 is mostly accounted for.

Another way to interpret the results of Buck et al. is to relate R_t for the α cluster to the radius of the valence orbits. There is about a 10% increase in the rms radius of the valence neutrons when they change from the ($0h_{9/2}$,$1f_{7/2}$,$1f_{5/2}$,$2p_{3/2}$,$2p_{1/2}$,$0i_{13/2}$) major shell below N=126 to the ($0i_{11/2}$,$1g_{9/2}$,$1g_{7/2}$,$2d_{5/2}$,$2d_{3/2}$,$3s_{1/2}$,$0j_{15/2}$) major shell above N=126. There should be a similar effect when the valence protons cross Z=82. The empirical Z dependence is shown on the right-hand side of Fig. 4. The lines which cross Z=82 are for

neutron numbers around ^{194}Pb (N=112) and surprisingly do not show a discontinuity at Z=82, perhaps because Z=82 is not a good magic number for these very light Pb isotopes. Other lines on the right-hand side of Fig. 4 start at Z=84 (the Po isotopes) and show about the same trend from Z=84 to Z=90 as for the neutron points between N=128 and N=140 on the left-hand side of Fig. 4. Thus, in summary, the comparison in Fig. 4b indicates a discontinuity in both N and Z centered only on the doubly magic nucleus ^{208}Pb. The orbit occupations of the valence protons and neutrons also influences the amount of proton-neutron correlation and hence the preformation probability. Quantitative calculations based on microscopic models have been difficult and controversial[6] and have thus far been limited mainly to the one case ^{212}Po α decay.

In summary, I have shown that the experimental values of $\mathrm{Log_{10}T_{1/2}(sec)}$ plotted vs $Z^{0.6}/\sqrt{Q_\alpha}$ fall on a nearly universal straight line. These systematics should be useful for extrapolations to more exotic nuclei and to superheavy nuclei. I also have shown that this behaviour comes out numerically from the semi-classical WKB approximation. It may be useful to consider whether or not there is any simpler underlying physical interpretation of this simple functional dependence of the decay rate on Z_d.

Acknowledgements

This work was supported in part by US National Science Foundation grant number PHY-90-17077.

Note added in proof

After completion of this paper I became aware of similar simple relations which have been proposed which are similar in spirit to mine but not the same in form. These are summarized in Ref 7. In particular, the form of Waptra et al.[8] can be fitted to the data

set considered here with the result, $\mathrm{Log_{10}T_{1/2}(sec)} = [(1.001Z_d + 51.89)/\sqrt{Q_\alpha}] - 51.37$, and with an rms deviation of 0.31. The form of Taagepera and Nurmia[9] and Keller and Munzel[10] can be fitted to the data set considered here with the result, $\mathrm{Log_{10}T_{1/2}(sec)} = 1.598[(Z_d/\sqrt{Q_\alpha}) - Z_d^{2/3}] - 19.94$, and with an rms deviation of 0.33.

Caption to Fig. 1

On the left-hand side (a), the experimental values for $\mathrm{Log_{10}T_{1/2}(sec)}$ are plotted vs $1/\sqrt{Q_\alpha}$, where the data for $\mathrm{T_{1/2}}$ and Q_α are taken from Ref 2. On the right-hand side (b), the experimental values for $\mathrm{Log_{10}T_{1/2}(sec)}$ are plotted vs $Z_d/\sqrt{Q_\alpha}$. The points for a given value of Z_d are connected by a lines.

Caption to Fig. 2

On the left-hand side (a), the experimental value for $\mathrm{Log_{10}T_{1/2}(sec)}$ are plotted vs $Z_d^{0.6}/\sqrt{Q_\alpha}$. The straight line represents a best fit to the data. On the right-hand side (b), the theoretical values for $\mathrm{Log_{10}T_{1/2}(sec)}$ from Eq. (1) are plotted vs $Z_d^{0.6}/\sqrt{Q_\alpha}$ and compared to the best fit line from Fig. 2a.

Caption to Fig. 3

Rms deviation of the straight-line fit to $\mathrm{Log_{10}T_{1/2}(sec)}$ vs $Z_d^x/\sqrt{Q_\alpha}$ as a function of the power x. The solid line is the fit to the experimental data and the dashed line is the fit to the semi-classical WKB calculation.

Caption to Fig. 4

On the top (a), the ratio of the experimental and theoretical decay rate for α decay (circles) is shown with the theoretical decay rate taken from Ref 2. On the left-hand side the points are plotted vs neutron number $N = N_d + 2$, and those for a given proton number $Z = Z_d + 2$ are connected by a line. On the right-hand side the points are plotted vs Z, and those for a given N value are connected by a line. On the bottom (b), the ratio of the experimental and theoretical decay rate for α decay is shown with the theoretical decay rate obtained from the present calculations with r_o=1.2 fm (circles) and r_o=1.1 fm (squares).

References:

1 H. Geiger and J. M. Nuttall, Phil. Mag. 22, 613 (1911); H. Geiger, Zeits. Physik 8, 45 (1921).

2 B. Buck, A. C. Merchant and S. M. Perez, Phys. Rev. Lett. 65, 2975 (1990); J. Phys. G17, 1223 (1991).

3 For example: S. S. M. Wong, "Introductory Nuclear Physics" (Prentice Hall, 1990).

4 For example: K. S. Toth et al., Phys. Rev. C45, 856 (1992); and Y. Hatsukawa, H. Nakahara and D. C. Hoffman, Phys. Rev. C42, 574 (1990).

5 B. A. Brown, C. R. Bronk and P. E. Hodgson, J. Phys. G10, 1683 (1984).

6 T. Fliessbach and S. Okabe, Z. Phys. A320, 289 (1985); A. Watt, D. Kelvin and R. R. Whitehead, J. Phys. G6, 31 (1980); and I. Tonozuka and A. Arima, Nucl. Phys. A323, 45 (1979).

7 D. N.Pomenaru and M. Ivascu, J. Physique 44, 791 (1983).

8 A. H. Wapstra et al. in "Nuclear Spectroscopy Tables", (North-Holland, Amsterdam) 1959.

9 R. Taagepera and M. Nurmia, Ann. Acad. Sci. Fenn. Ser. A78, (1961).

10 K. A. Keller and H. Z. Munzel, Z. Physik 255, 419 (1972).

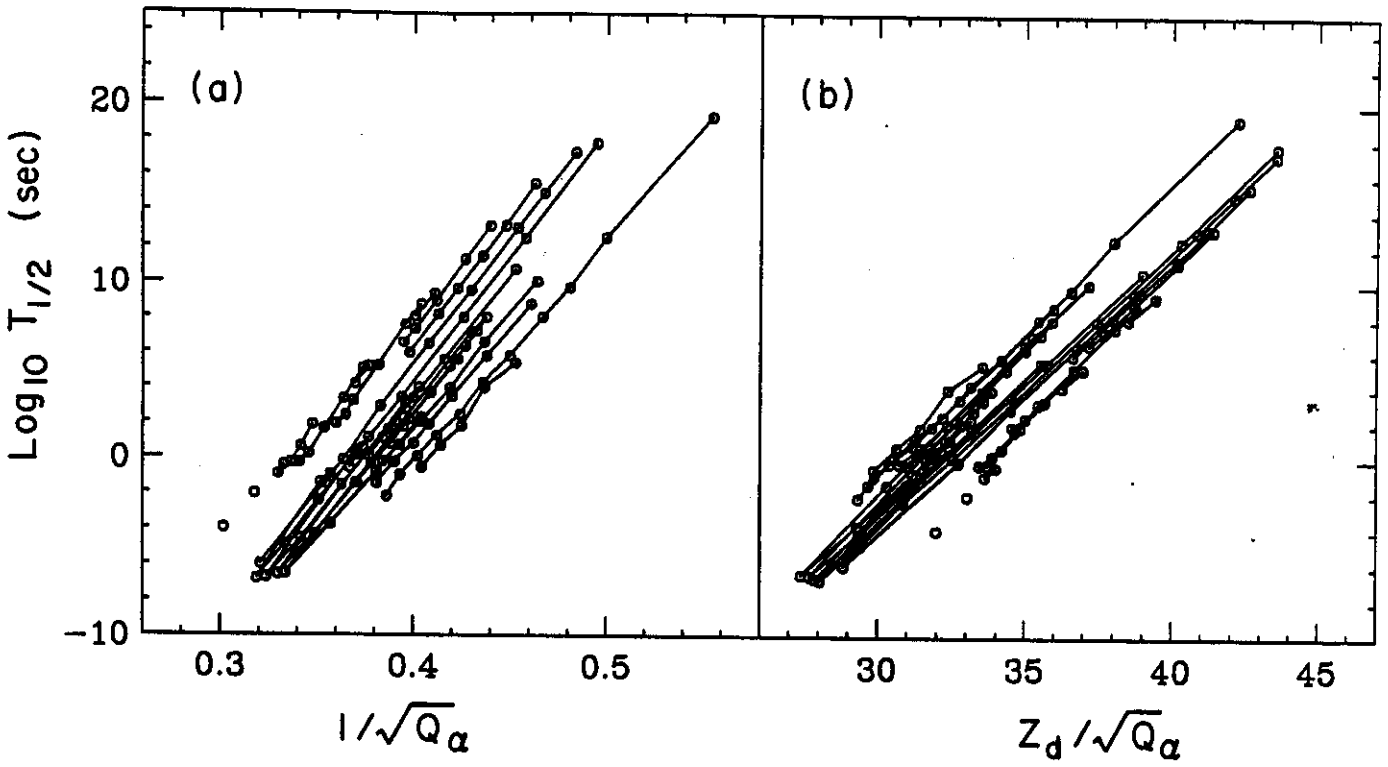
(a)
(b)
20
10
0
−10
0.3
0.4
0.5
30
35
40
45
$\mathrm{Log_{10}}\ T_{1/2}$ (sec)
$1/\sqrt{Q_\alpha}$
$Z_d/\sqrt{Q_\alpha}$

Fig. 1

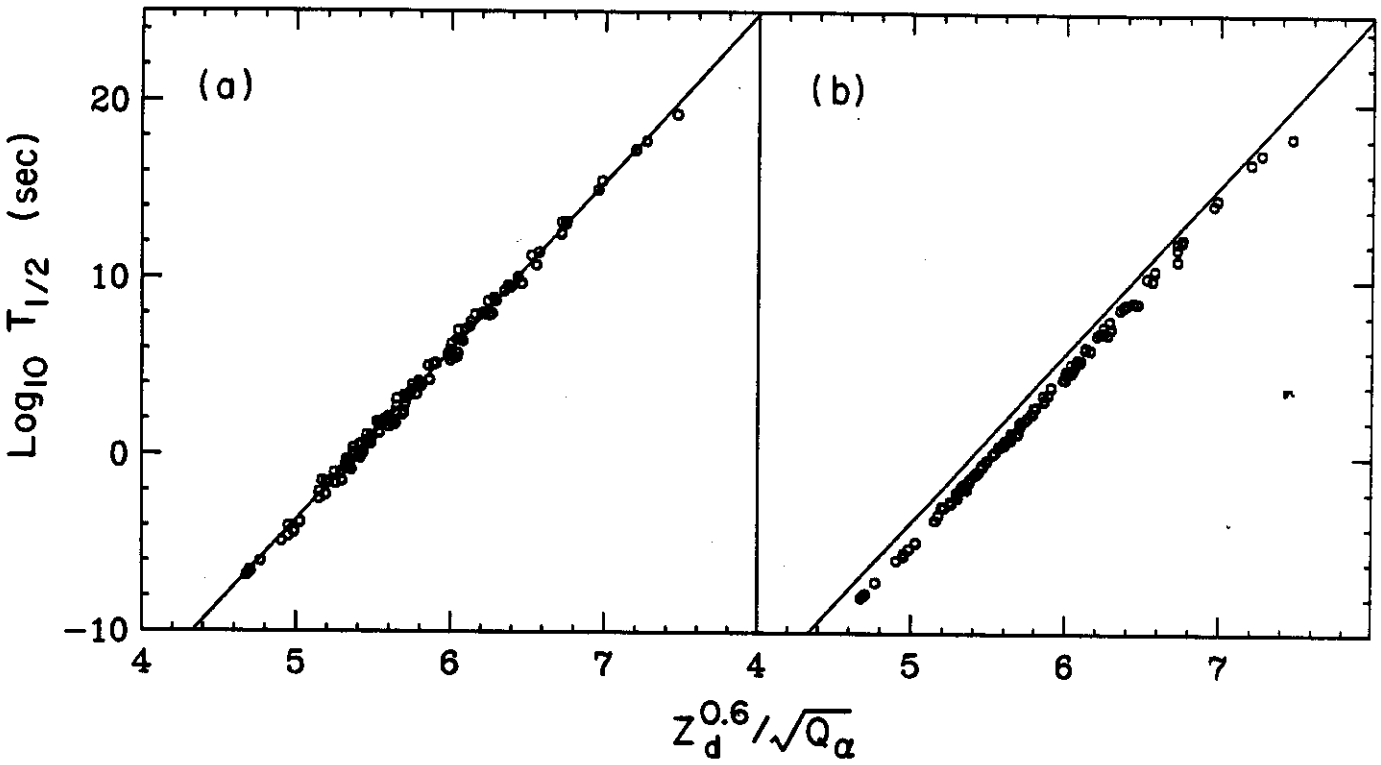

Fig. 2

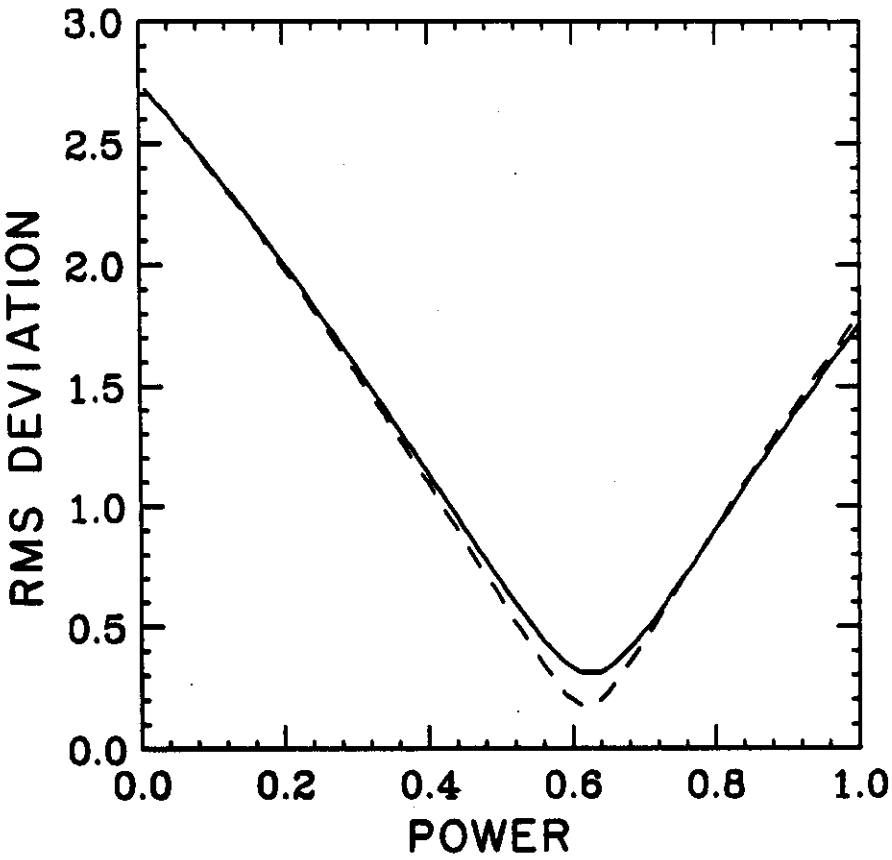

Fig. 3

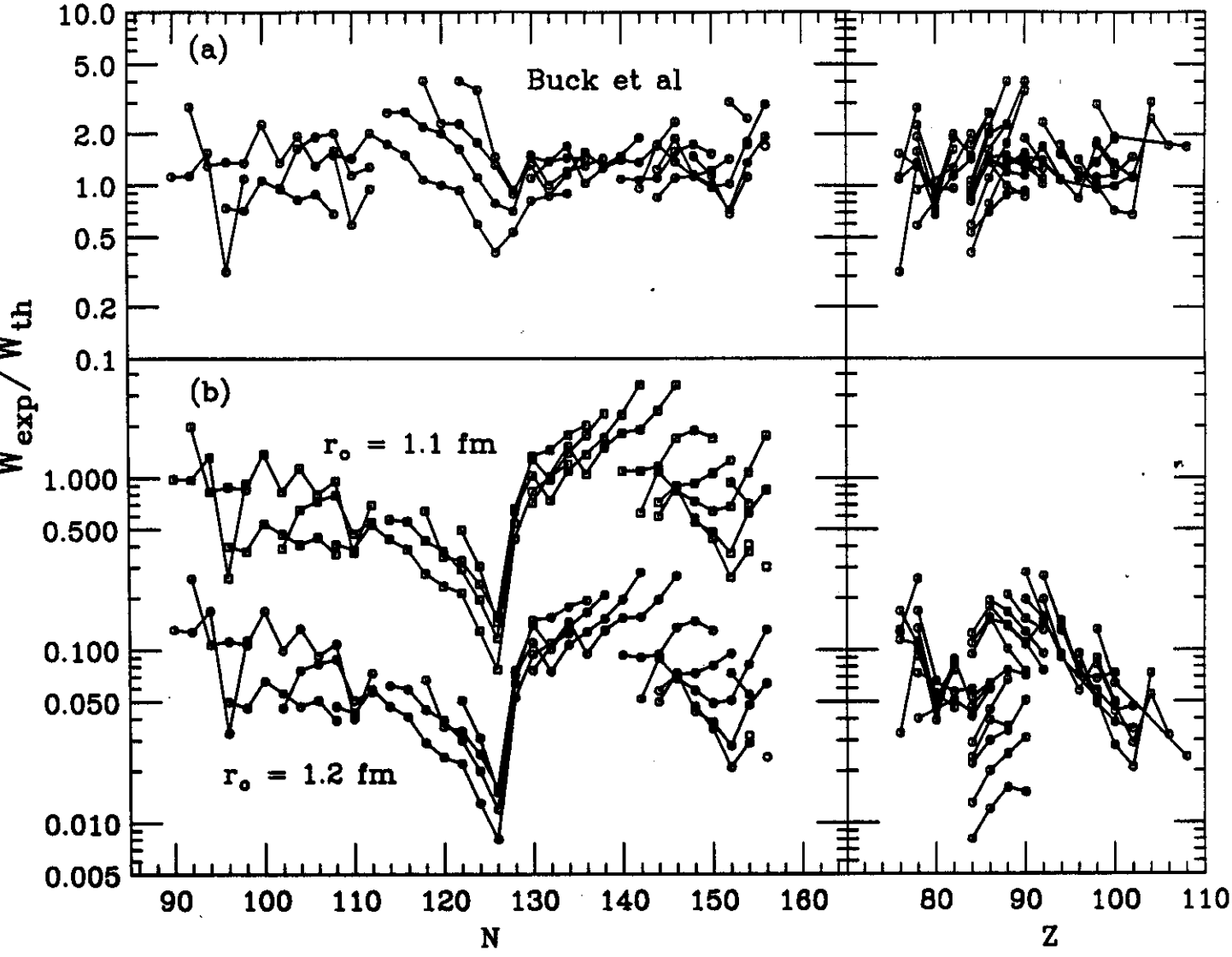

Fig. 4